

## Kinetic roughening of amorphous $\text{Zr}_{65}\text{Al}_{7.5}\text{Cu}_{27.5}$ films investigated *in situ* with scanning tunneling microscopy

B. Reinker, M. Moske, and K. Samwer

*Institut für Physik, Universität Augsburg, D-86135 Augsburg, Germany*

(Received 13 May 1997)

The isotropic nature of metallic glasses, lacking in long-range structural order, suggests an advantage for surface growth studies. In the present work the surface topography of vapor quenched amorphous  $\text{Zr}_{65}\text{Al}_{7.5}\text{Cu}_{27.5}$  films is investigated *in situ* with scanning tunneling microscopy. The development of surface morphology on mesoscopic length scales is analyzed with respect to an increasing film thickness. Vertical roughness and in-plane correlation are statistically analyzed by a height-height correlation function. With film thickness less than 30 nm, the surface roughness evolves with a growth exponent  $\beta$  of approximately 0.2. Above a film thickness of 30 nm we find strong deviations from a self-affine scaling behavior. A roughening transition is observed, at which the lateral size of the characteristic surface structures converges to a maximum value. Moreover, the size of the uniform surface structures is increased with elevated substrate temperature during film deposition. We show that the in-plane size of these structures is governed by surface diffusion. In an approximation, neglecting nonlinear corrections, the experimental results are analyzed with respect to a growth model proposed by Wolf and Villain [Europhys. Lett. **13**, 389 (1990)]. [S0163-1829(97)07139-7]

### I. INTRODUCTION

Kinetic roughening<sup>1-3</sup> has attracted great interest during the past few years. Due to common growth conditions (e.g., low temperatures and high deposition rates) in thin-film applications, the description of film growth by “near-equilibrium” growth conditions is no longer valid. In contrast, a rather restricted atomic mobility will be responsible for the development of the surface morphology in such “far-from-equilibrium” growth phenomena. Under these conditions fluctuations become relevant. In this context one of the most challenging problems is the understanding of the dynamics of rough interfaces.

Approaches to this research area are analytical theories, including modeling the dynamics of an interface with a stochastic differential equation (Langevin equation<sup>3</sup>) in the form

$$\frac{\partial z(\vec{r}, t)}{\partial t} = -\vec{\nabla} \cdot \vec{j}(\vec{r}, t) + \eta(\vec{r}, t), \quad (1)$$

based on mass conservation. In this type of equation  $\vec{j}(\vec{r}, t)$  is responsible for the mass transport parallel to the surface  $z(\vec{r}) = h(\vec{r}) - \bar{h}$ , with  $\vec{r} = (x, y)$  and  $\bar{h}$  being the average film thickness. According to the random nature of molecular-beam deposition, a noise term  $\eta$  with Gaussian distribution is introduced, which will be responsible for surface roughening. In the absence of any lateral mass transport, the surface is uncorrelated and the roughness  $\sigma$  will evolve proportional to the square root of the film thickness, provided the deposition is at constant rate  $n = \bar{h}/t$ . Any relaxation mechanism, introduced in continuum theory approaches, will modify this power law of roughening.

A basic assumption for all these models is the isotropic nature of the growing interface. Dealing with molecular-beam growth, a crystalline anisotropy with the formation of facets is undesirable. Therefore, systems that condense into

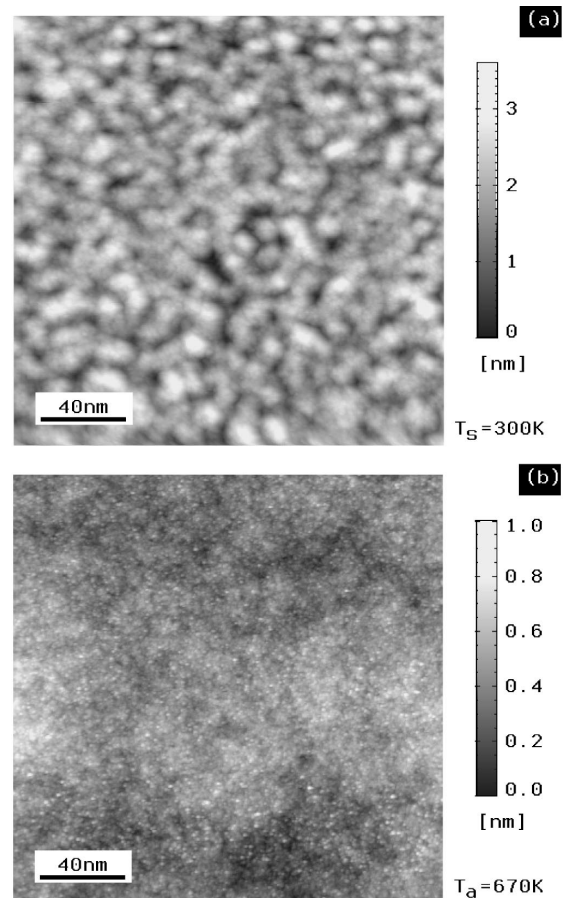


FIG. 1. Growth-induced surface structures of a  $\bar{h} = 100$  nm film deposited at temperature  $T_s = 300$  K (a) are relaxed during an annealing step at  $T_a = 670$  K for 10 min (b). The STM image shows only the intrinsic roughness, corresponding to the atomic disorder of the amorphous alloy.

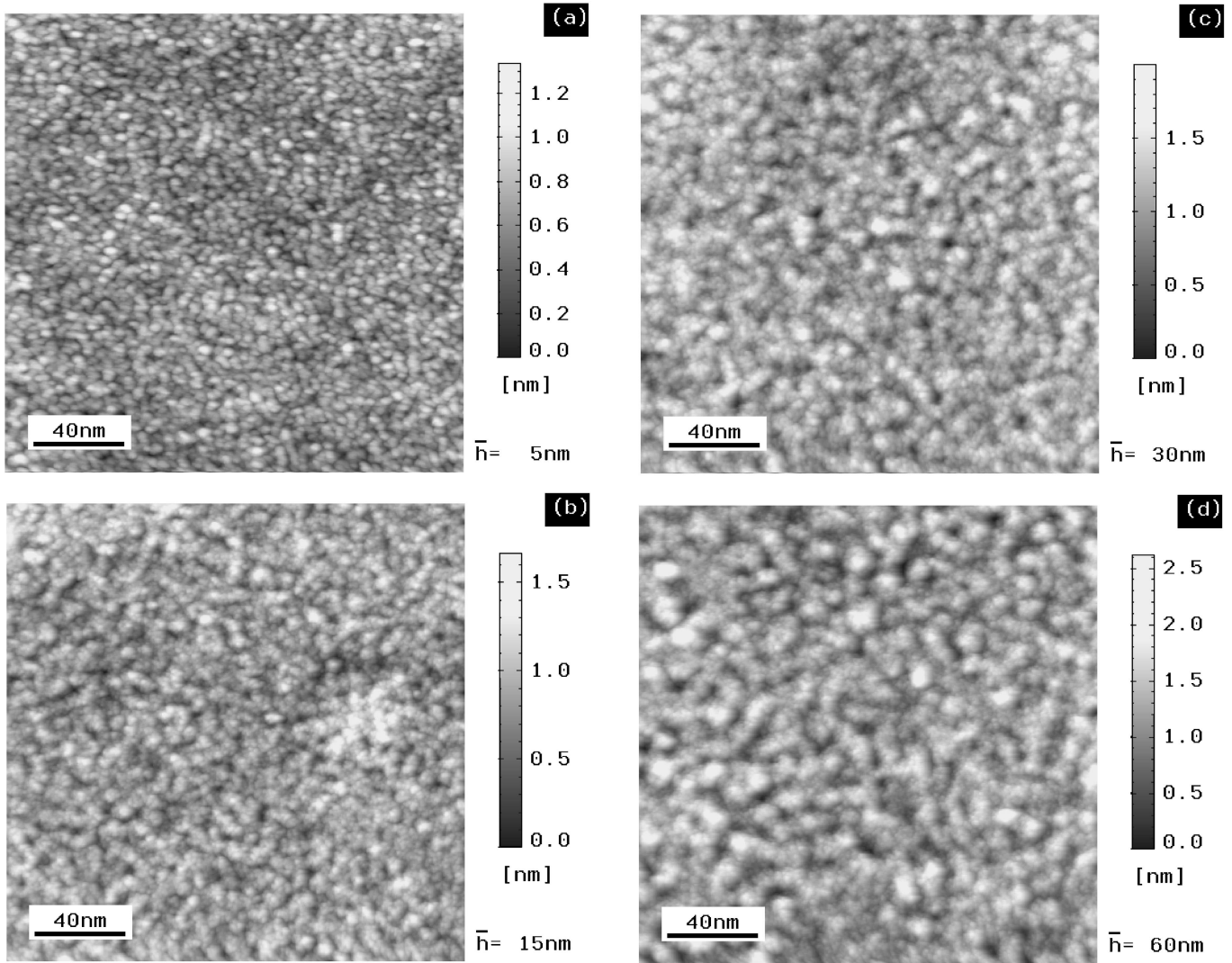


FIG. 2. Growth sequence showing the evolution of surface morphology with increasing film thickness  $\bar{h}$  at (a) 5 nm, (b) 15 nm, (c) 30 nm, (d) 60 nm, (e) 120 nm, (f) 240 nm, and (g) 480 nm. The films are deposited at substrate temperature  $T_s = 300$  K. All STM images are scanned with the same parameters.

an amorphous state have the advantage of comparing the evolution of the interface during growth with such models.

Experimentally, film growth can be studied with small-angle x-ray scattering methods,<sup>4,2</sup> scanning tunneling microscopy (STM), and atomic force microscopy. In an earlier paper<sup>5</sup> it was shown that the results of both complementary techniques compare well for an amorphous ZrCo alloy we investigated.

Solving the growth equation one obtains the height-height correlation of the interface, which provides a link between the model and the experiment. From the STM images, recorded in a constant current mode, the height-height correlation function<sup>6,7</sup>

$$C(R) := \langle z(\vec{r})z(\vec{r} + \vec{R}) \rangle_{r,R} \quad (2)$$

is calculated from the image data. Therein  $\langle \rangle_{r,R}$  denotes the average over all pairs of surface points, separated horizontally by distance  $R$ . In addition to that quantitative information, one obtains a qualitative impression of surface mor-

phology. Alternatively, the representation of the height-difference correlation function<sup>4,8</sup>

$$H(R) := \langle [z(\vec{r}) - z(\vec{r} + \vec{R})]^2 \rangle_{r,R} \quad (3)$$

can be derived as commonly used for growth studies in the framework of fractal concepts.

In this work we present *in situ* STM investigations on amorphous  $\text{Zr}_{65}\text{Al}_{7.5}\text{Cu}_{27.5}$  films.<sup>9,10</sup> The ternary alloy belongs to a special class of metallic glasses with an extended supercooled liquid region,<sup>11,12</sup> the temperature range between glass transition temperature  $T_g$  and crystallization temperature  $T_x$ . This in fact indicates an increased stability against nucleation and crystallization for temperatures above  $T_g$  and therefore allows studies in the undercooled liquid.

## II. EXPERIMENTAL DETAILS

ZrAlCu films, with the composition of  $\text{Zr}_{65}\text{Al}_{7.5}\text{Cu}_{27.5}$  within  $\pm 2$  at. % for each component, are cocondensed in

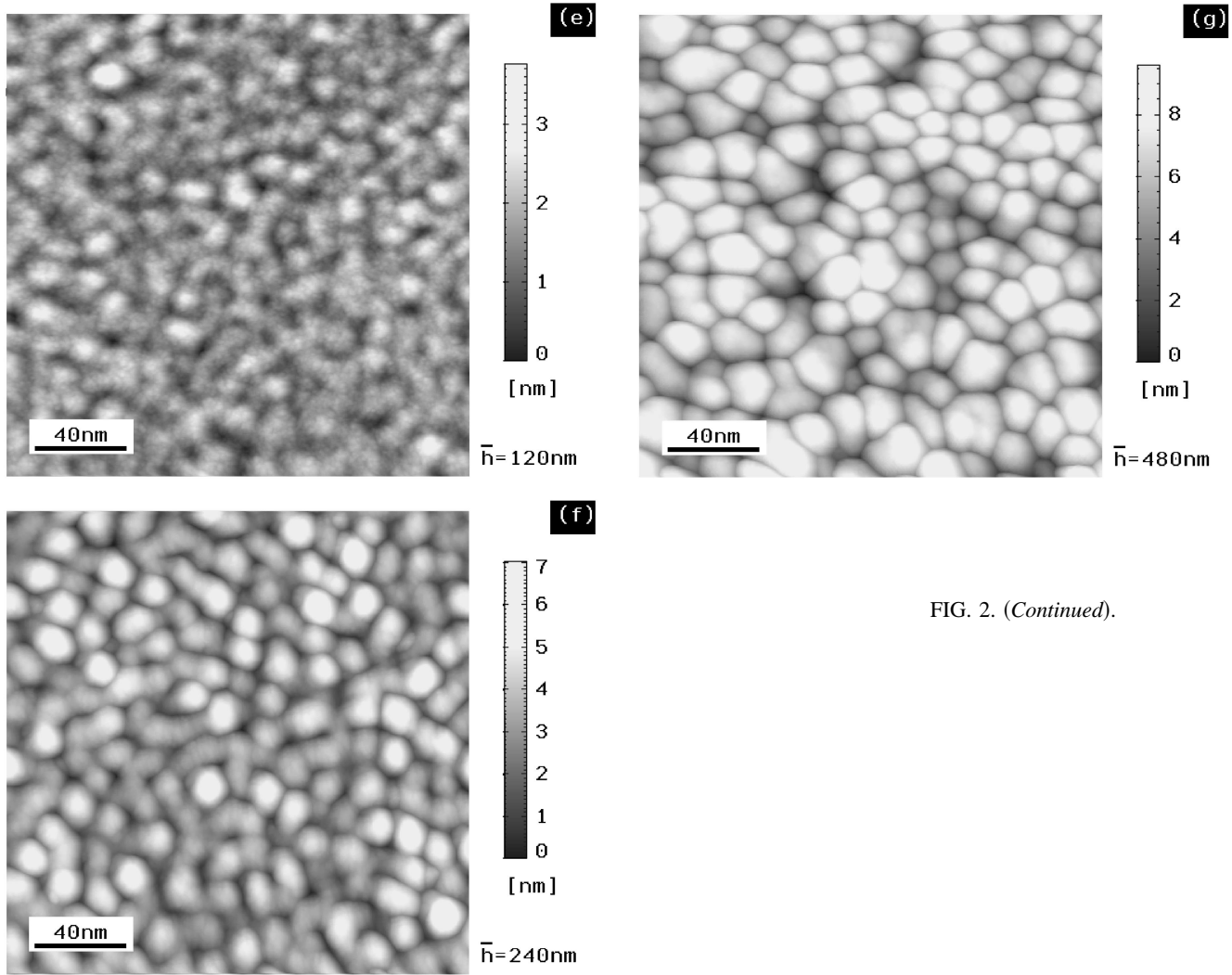


FIG. 2. (Continued).

ultrahigh vacuum (UHV) onto silicon substrates by three rate-controlled electron-beam evaporators with a total deposition rate of 0.79 nm/s. The initial roughness of the silicon wafers, covered with 0.5  $\mu\text{m}$  of thermal oxide, is about 0.29 nm as determined from a small-angle x-ray-diffraction pattern. During deposition the substrate is rotating to avoid concentration gradients in the film. The tilting angle between crucibles and substrates is about 10°. Shadowing effects are neglected for the films we investigated.

The surface morphology of the films is analyzed with scanning tunneling microscopy (UHV-STM1, Omicron) in the constant current mode using electrochemically etched tungsten tips. Tunneling conditions of typically  $U_t = 1.0$  V and  $I_t = 1.0$  nA are chosen for scanning a sample area of  $200 \times 200$  nm<sup>2</sup> with a step size of 0.5 nm. In addition, the amorphous nature of the films is verified *ex situ* by x-ray diffraction.

### III. RESULTS

Thin films of ZrAlCu show smooth hill-like surface structures [Fig. 1(a)], similar to those known from other amorphous alloys.<sup>13</sup> The so-called mesoscopic surface roughness is relaxed after annealing the amorphous films to temperatures above the glass transition  $T_g$  of about 650 K, as shown

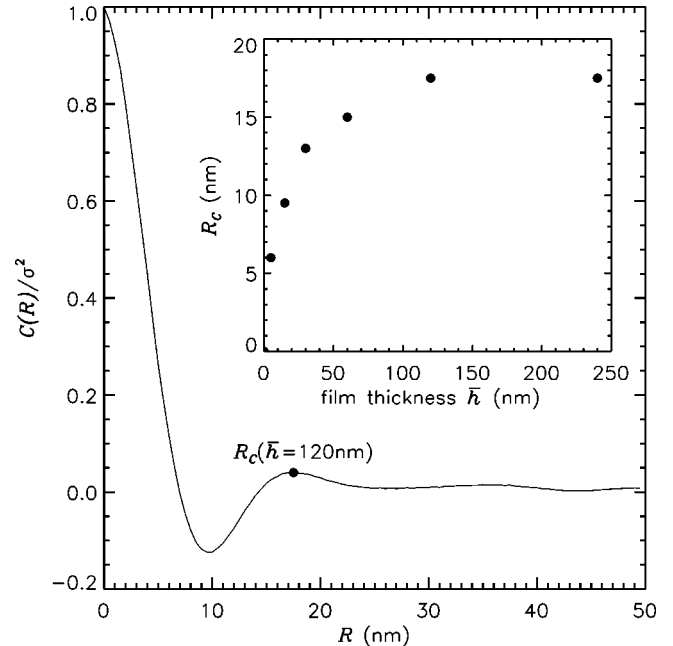


FIG. 3. Height-height correlation function  $C(R)/\sigma^2$  (normalized). In the inset the determined correlation length  $R_c$  is plotted versus film thickness  $\bar{h}$ .

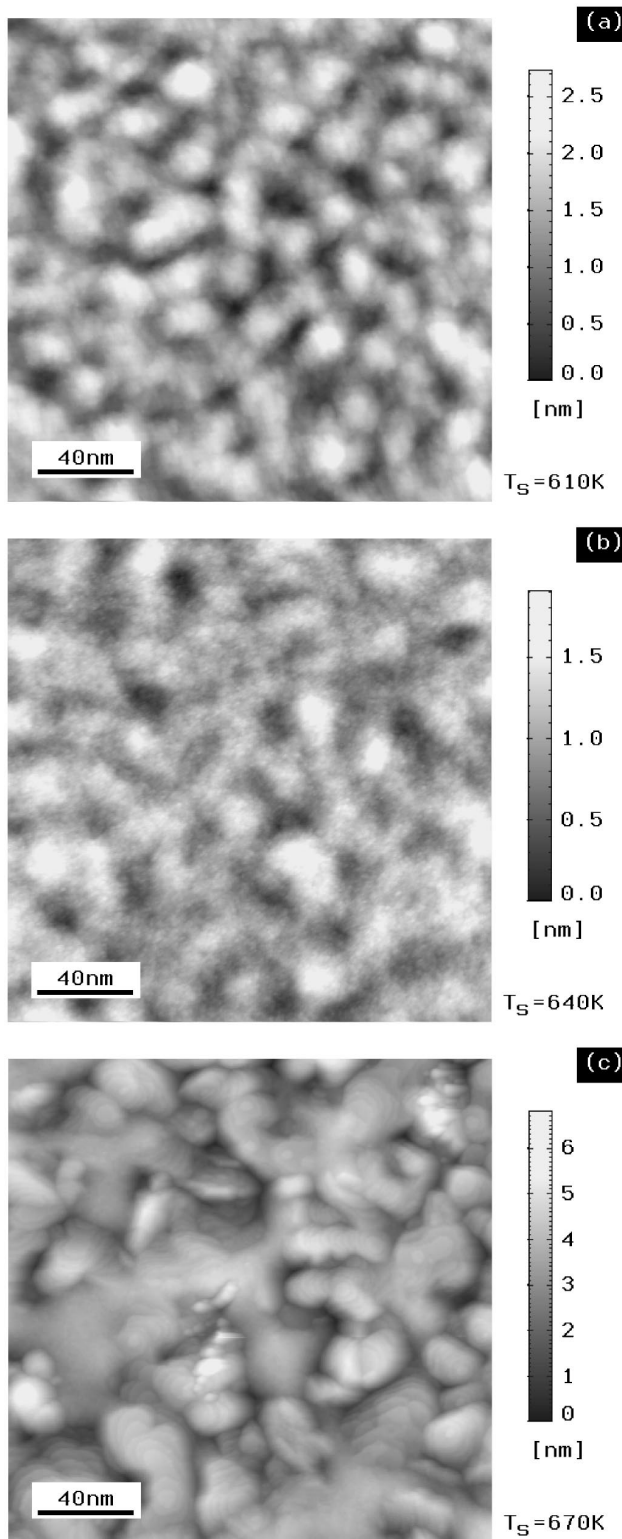


FIG. 4. STM images of ZrAlCu films with  $\bar{h} = 100$  nm deposited at different substrate temperatures  $T_s$ : (a) 600 K, (b) 640 K, and (c) 670 K (crystalline).

in Fig. 1(b). For further details see Ref. 14. Such a relaxed surface with rms roughness of about 0.1 nm, due to the viscous flow of the film above  $T_g$ , is the starting point for a growth sequence of the same amorphous alloy, as shown below.

First we will focus on the evolution of the amorphous

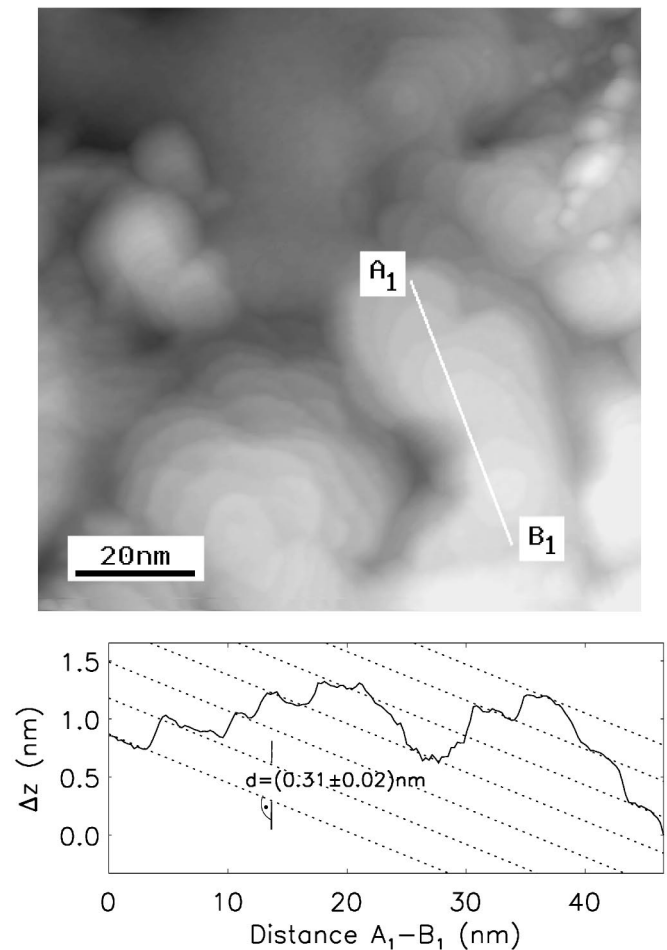


FIG. 5. Magnification of the area of the bottom left corner of Fig. 4(c) and profile along the distance  $A_1-B_1$ , showing the step structure of several atomic layers.

surface structures during film growth. In Fig. 2 the growth sequence of an amorphous ZrAlCu film is shown in representative STM topographs. For this growth study, with the substrate at temperature  $T_s = 300$  K, we have interrupted the deposition at several thickness stages for monitoring the surface morphology with STM. With increasing film thickness  $\bar{h}$  the lateral size of the uniform surface structures increases. After deposition of 120 nm, a maximum size of about 18 nm in the lateral direction is reached, as determined from  $C(R)$ , shown in Fig. 3. With further deposition surface roughening is increased, up to a film thickness of about 300 nm, where a stationary state for surface roughness  $\sigma = \sqrt{C(0)}$  is reached for the frames  $200 \times 200$  nm<sup>2</sup> investigated [see Fig. 2(g)]. Alternatively, the same thickness-dependent values of rms roughness  $\sigma$  can be determined from a Gaussian fit to the height-distribution data of the STM images.

It is remarkable that at a film thickness of about 120 nm surface structures of the same size and shape as shown in Fig. 1(b) are observed. In a statistical manner both Figs. 1(b) and 2(e) are equivalent, i.e., the dynamics of surface morphology is independent of the initial substrate features.

Additionally, we have investigated the dependence of surface morphology due to different substrate temperatures  $T_s$  during deposition. The STM images are presented in Fig. 4. Up to temperatures near the glass transition  $T_g$  the amor-

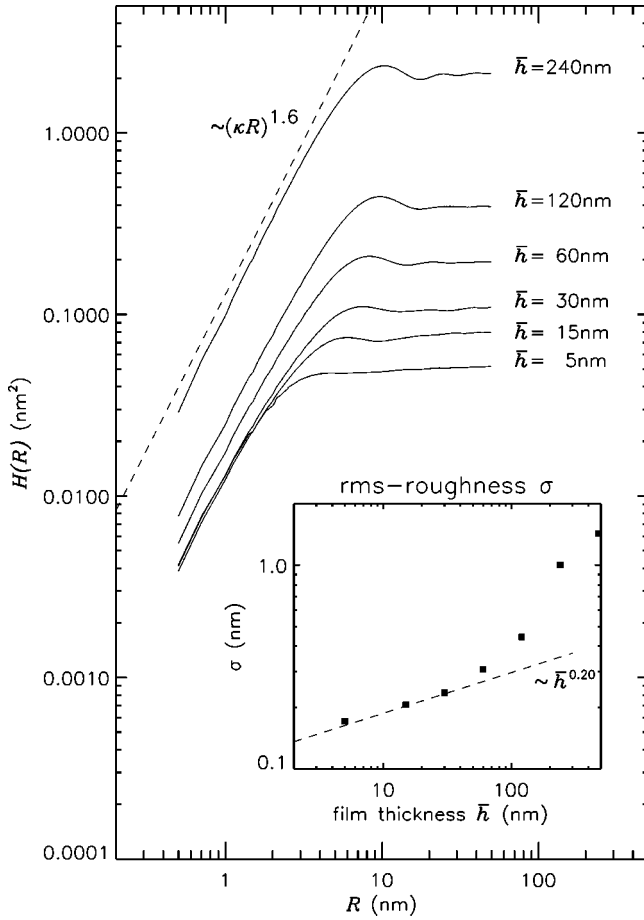


FIG. 6. Height-difference correlation function  $H(R)$  and surface roughness  $\sigma$  (inset) depending on film thickness in a log-log plot.

phous hill-like structures are smeared out, i.e., the lateral size is increased while surface roughness is decreased. At substrate temperatures above  $T_g$  the atomic mobility is sufficiently high and the film crystallizes during deposition [Fig. 4(c)]. Small crystallites with flat terraces of step size  $3.1 \pm 0.1 \text{ \AA}$  are observed (Fig. 5), corresponding to the lattice parameter  $a = 3.2204 \text{ \AA}$  of bct- $\text{Zr}_2\text{Cu}$ .<sup>15</sup> The crystalline phase is also verified with x-ray diffraction.

#### IV. DISCUSSION

The question whether or not the surface is self-organized can be answered by presenting the height-difference function  $H(R)$  with log-log scales. From Fig. 6 it is shown that up to a film thickness of about 30 nm the surface shows dynamic scaling behavior for in-plane correlations and vertical fluctuations (see, e.g., Refs. 2 and 3). At small distances  $R$  the correlation function  $H(R)$  will fit to  $(\kappa R)^{2\alpha}$ , where  $\kappa$  indicates an average surface slope.<sup>16</sup> The roughness exponent  $\alpha = 0.8$  is independent of film thickness, while the growth exponent  $\beta = 0.2$  is only defined for the early stages of film growth. With a further increase of film thickness,  $\kappa$  becomes thickness dependent (Table I), indicating the roughening transition mentioned above. The vertical direction of the hill-like surface structures grows faster than the lateral ones.

The results for films grown at elevated temperatures suggest that surface relaxation is governed by a diffusive surface current. In a growth model proposed by Wolf and Villain<sup>17</sup>

TABLE I. Results from  $C(R)$  and  $H(R)$  calculated at different thickness stages  $\bar{h}$ .

Film thickness $\bar{h}$ (nm)	Correlation length $R_c$ (nm)	rms roughness $\sigma$ (nm)	Average surface slope $\kappa$ ( $\text{nm}^{-1}$ )
0		0.10	
5	6.0	0.17	0.064
15	9.5	0.21	0.064
30	13.0	0.24	0.064
60	15.0	0.31	0.079
120	17.5	0.44	0.1
240	17.5	1.00	0.24
480		1.43	

the surface current is driven by differences in surface chemical potential  $\mu$ , which is set proportional to local surface curvature.<sup>18,19</sup> For small surface gradients it can be approximated by  $\mu \propto \nabla^2 z(\vec{r})$ . Thus, due to the absence of desorption (for substrate temperatures  $T_s \leq 650 \text{ K}$  a supersaturation of  $10^{10}$  or greater is estimated) Eq. (1) is rewritten as<sup>17,20</sup>

$$\frac{\partial z(\vec{r}, t)}{\partial t} = -D_L \nabla^4 z(\vec{r}, t) + \eta(\vec{r}, t), \quad (4)$$

with  $D_L$  being the coefficient for surface diffusion. Assuming self-affine growth, a scaling behavior is expected, depending on the system dimension. In three dimensions the interface evolves with  $\alpha = 1$  and  $\beta = 0.25$ . This may fit to the experimental results for the early stages of  $\text{ZrAlCu}$  film growth observed by STM.

The solution of the linear Langevin equation in Eq. (4), apart from scaling concepts, gives the height-height correlation function. In reciprocal space, the Fourier transformation of the height-height correlation has the form

$$C(q) = \langle |z(\vec{q}, t)|^2 \rangle_q \propto \frac{D_V}{D_L q^4} (1 - e^{-2D_L q^4 t}). \quad (5)$$

Therein the parameter  $D_V$  is a constant depending on evaporation conditions, such as deposition rates. Deposition with random nature will generate a ‘‘white’’ spectrum of surface disturbances in Fourier space. Due to a limited adatom mobility disturbances with spatial frequencies lower than  $q_c \approx (D_L t)^{-1/4}$  will not participate in surface relaxation, i.e., the corresponding long-range corrugations in real space are responsible for surface roughness. Frequency modes with a periodicity higher than  $q_c$  are ‘‘damped out’’ with a power of  $q^{-4}$ . In Fig. 7 two calculated  $C(q)$  curves are presented, showing the predicted power law. Moreover, with higher substrate coverage a peak is evolving in the region of  $q_c$ .

The above description considers only linear effects for the growth front dynamics and should be regarded as reasonable approximation. In fact, the results differ from a self-affine scaling behavior, as observed for film growth with a mode selection process involved. Nevertheless, nontrivial relaxation patterns will only lead to small deviations in the region of the ‘‘cutoff’’ frequency  $q_c$  (see Fig. 7). Therefore, the

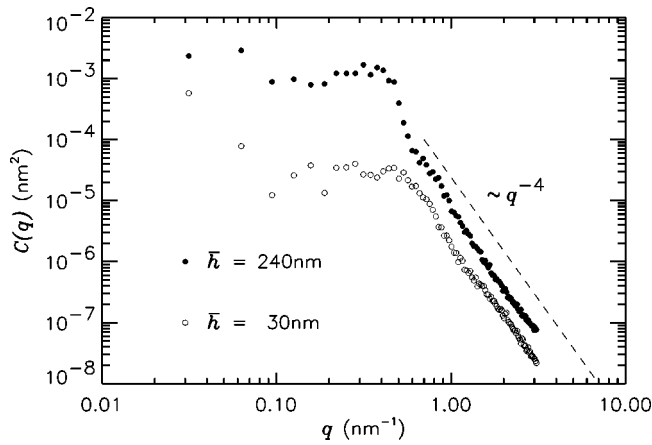


FIG. 7. Height-height correlation function  $C(q)$ . For surface corrugations with periodicity greater than  $q_c$  the shape follows a power law of  $1/q^4$ .

average size of the surface structures, in one approximation, corresponds to  $R_c \approx 2\pi/q_c$ , i.e., the magnitude of  $R_c$  is predominated by the  $\nabla^4 z(\vec{r})$  term of surface diffusion. Assuming  $D_L = D_0 \exp\{-E_D/kT_s\}$ , with  $D_0$  to be constant for the temperatures investigated, it is possible to estimate an average activation energy  $E_D$  for surface diffusion. In Fig. 8 the logarithm of  $R_c$  is plotted versus  $1/T_s$  for substrate temperatures below  $T_g$ . From linear regression of the data points an activation energy of  $E_D = 0.52$  eV is determined. This value gives at least the correct magnitude of activation energies for adatom mobility on metal surfaces.

As mentioned above, with increasing film thickness, accompanied by an increase of surface roughness, nonlinear effects, e.g., according to the experimental conditions of film growth, become more and more relevant. For sputter deposited films, for example, with an isotropic particle flux incoming from all directions, shadowing enhances local instabilities. In a continuum approach such effects can be taken into account by modulating the deposition rate with respect to an exposure angle, depending on the surrounding at each surface point.<sup>21</sup> In our case, the molecular beam is directed more or less perpendicular to the substrate, such that film growth depends only on local surface properties. A modified model, including geometrical corrections, will be discussed elsewhere.<sup>22</sup> The comparison of the experimental results with simulated surfaces, generated from more generalized continuum models, is part of the present investigation.

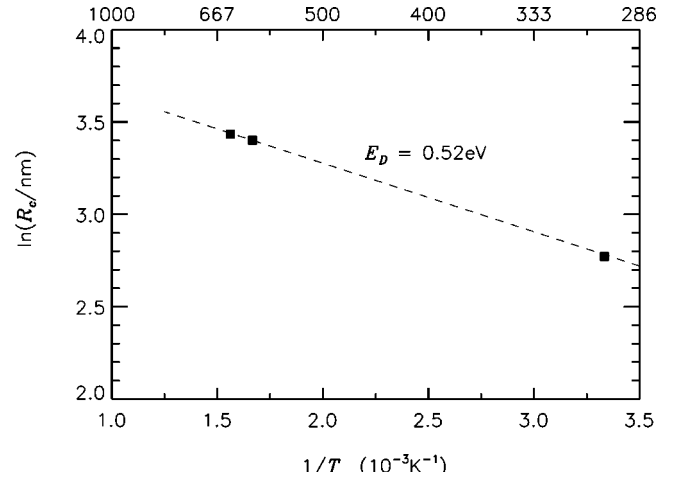


FIG. 8.  $\ln R_c$  (nm) vs  $1/T_s$ . From the slope, determined by linear regression, an average activation energy for surface diffusion  $E_D = 0.52$  eV is detected.

## V. CONCLUSION

In conclusion, we can state that amorphous metals, for example, ZrAlCu, are favorite systems for growth studies in the framework of kinetic roughening due to their isotropic surface features. For the early stages of film growth, starting with a flat surface, the evolution of surface morphology seems to be self-organized. With increasing surface roughness during film growth a roughening transition is observed, with stabilization of a uniform size of surface structures involved. The lateral size  $R_c$  of the hill-like surface structures depends on the adatom mobility. For films deposited at elevated substrate temperatures,  $R_c$  is shifted towards higher values. Describing the evolution of these amorphous films in the context of stochastic growth equations, the lateral size of the surface structures is predominated by the  $\nabla^4 z(\vec{r})$  surface diffusion term. Thus, from the development of  $R_c$  with increasing substrate temperature, we are able to estimate an average activation energy for surface diffusion.

## ACKNOWLEDGMENTS

The authors are indebted to S. Mayr, who carries on the experimental work, for additional results, and H. Geisler for his expert advice in film preparation. Appreciation is expressed to U. Herr for valuable discussions.

<sup>1</sup>Dynamics of Fractal Surfaces, edited by F. Family and T. Vicsek (World Scientific, Singapore, 1991).

<sup>2</sup>H.-N. Yang, G.-C. Wang, and T.-M. Lu, *Diffraction from Rough Surfaces and Dynamic Growth Fronts* (World Scientific, Singapore, 1993).

<sup>3</sup>A. L. Barabasi and H. E. Stanley, *Fractal Concepts in Surface Growth* (Cambridge University Press, Cambridge, 1995).

<sup>4</sup>S. Sinha, E. Sirota, S. Garoff, and H. Stanley, *Phys. Rev. B* **38**, 2297 (1988).

<sup>5</sup>T. Salditt *et al.*, *Europhys. Lett.* **32**, 331 (1995).

<sup>6</sup>J. Ogilvy, *Theory of Wave Scattering From Random Rough Surfaces* (IOP, London, 1991).

<sup>7</sup>G. Rasigni *et al.*, *Phys. Rev. B* **27**, 819 (1983).

<sup>8</sup>C. Thompson *et al.*, *Phys. Rev. B* **49**, 4902 (1994).

<sup>9</sup>A. Inoue, T. Zhang, and T. Masumoto, *J. Non-Cryst. Solids* **150**, 396 (1992).

<sup>10</sup>A. Inoue *et al.*, *Mater. Sci. Eng. A* **178**, 255 (1994).

<sup>11</sup>T. Masumoto, *Sci. Rep. Res. Inst. Tohoku Univ. A* **39**, 91 (1994).

<sup>12</sup>W. L. Johnson, in *Science and Technology of Rapid Solidification and Processing Technologies*, Vol. 278 of *NATO Advanced*

- Study Institute, Series E*, edited by M. A. Otooni (Plenum, New York, 1994), p. 25.
- <sup>13</sup>B. Reinker, M. Moske, H. Geisler, and K. Samwer, in *Evolution of Thin Film and Surface Structure and Morphology*, edited by B. G. Demczyk *et al.*, MRS Symposia Proceedings No. 355 (Materials Research Society, Pittsburgh, 1995), p. 601.
- <sup>14</sup>B. Reinker, H. Geisler, M. Moske, and K. Samwer, *Thin Solid Films* **275**, 240 (1996).
- <sup>15</sup>*Powder Diffraction File, Inorganic and Organic*, edited by JCPDS Internal Centre of Diffraction Data (JCPDS, Swarthmore, 1974–1988), Vols. 1–38.
- <sup>16</sup>T.-M. Lu, H.-N. Yang, and G.-C. Wang, in *Fractal Aspects of Materials*, edited by F. Family *et al.*, MRS Symp. Proc. No. 367 (Materials Research Society, Pittsburgh, 1995), p. 283.
- <sup>17</sup>D. Wolf and J. Villain, *Europhys. Lett.* **13**, 389 (1990).
- <sup>18</sup>W. Mullins, *J. Appl. Phys.* **28**, 333 (1957).
- <sup>19</sup>W. Mullins, *J. Appl. Phys.* **30**, 77 (1959).
- <sup>20</sup>S. Das Sarma and P. Tamborenea, *Phys. Rev. Lett.* **66**, 325 (1991).
- <sup>21</sup>R. Karunasiri, R. Bruinsma, and J. Rudnick, *Phys. Rev. Lett.* **62**, 788 (1989).
- <sup>22</sup>M. Moske (unpublished).